

Mass transfer to tubular electrodes. Part 2: CE process

Tejwant Singh^a, Rajinder Pal Singh^a and Jatinder Dutt^b

^a *Department of Mathematics and Statistics, Punjab Agricultural University, Ludhiana 141004, India*

^b *Department of Chemical Engineering and Technology, Punjab University, Chandigarh 160014, India*

Received 9 September 1996; revised 15 December 1997

The kinetic equations for an electrochemical process consisting of a homogeneous first-order chemical reaction followed by electron transfer at the electrode surface are solved numerically, for linear sweep voltammetry under hydrodynamical conditions in a tubular electrode. Models for both the cases involving reversible as well as irreversible electrode charge transfer reaction are investigated. The influence on current–potential voltammograms of the experimentally measurable parameters like the potential scan rate, axial flow rate and chemical equilibrium parameter is examined and depicted graphically.

1. Introduction

The role of mathematical models in the investigation of mechanism of electrochemical reaction has widely developed, during the last three decades, to become an invaluable tool [9]. It has made possible to extract relevant parameters, for example, rate constants, equilibrium constants, etc., for complex reaction schemes where complexity arises due to the coupling of chemical reaction for multiple electrode charge transfer reactions. Though the method of theoretical modelling is less general than the direct solution of kinetic equations, i.e., by the finite difference/finite element approach [10], it usually converts the kinetic partial differential equations into corresponding integral equations and solves the later by computers [17]. It enables the expression for the influence of reaction parameters such as the potential scan rate, bulk concentrations, diffusion coefficients in a semianalytical way [1,3].

Among various electrochemical transient techniques, linear sweep voltammetry/cyclic voltammetry are the most effective in resolving complex electrode reaction mechanisms [4]. However, the successful use of these techniques depends largely on theoretical modelling studies which provide a formation for the description of current potential curves. In simple kinetic cases, analytic expressions for the voltammograms are available, complex electrode reaction mechanisms require numerical calculations [7,8,19].

Number of theoretical and experimental studies [5,11,13–16] have been reported concerning hydrodynamic voltammetry at an electrode which forms a part of the wall of a cylindrical tube or a rectangular channel. The electrochemical flow cells have

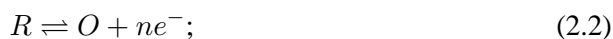
some advantages over quiescent conditions [2]. The investigations of the electrochemical process involving complexity of coupled chemical reaction with electrode charge transfer reactions in hydrodynamic electrode are reported by many workers [6,12,18,20].

In the recently reported work [21], the authors have studied the EC processes for hydrodynamic linear sweep voltammetry in which homogeneous reversible chemical reactions are following reversible charge transfer reactions. In the present paper, the effects of homogeneous reversible chemical reactions which are preceding the charge transfer reactions under hydrodynamical conditions at the tubular electrode are theoretically investigated. The effects of experimentally measurable parameters, e.g., the potential scan rate, axial flow rate, chemical equilibrium constant on the current potential voltammograms of linear sweep voltammetry are studied and shown graphically. The limiting cases of this general model reduces to simple kinetic cases as already reported.

2. Formulation of the problem

The process in which first-order homogeneous reversible chemical reaction is followed by electrode charge transfer ((a) reversible, (b) irreversible) is generalized as

(a)



(b)



where k' is the first-order rate constant, k_f and k_b are forward and backward chemical reaction rate constants.

The mathematical model representing the above processes in which the reactants are flowing through a tubular electrode, lamilarly, is

$$\frac{\partial C_Z}{\partial t} + v_a(r) \frac{\partial C_Z}{\partial z} = D_Z \left[\frac{\partial^2 C_Z}{\partial r^2} + \frac{1}{r} \frac{\partial C_Z}{\partial r} \right] - k_f C_Z + k_b C_R, \quad (2.5)$$

$$\frac{\partial C_R}{\partial t} + v_a(r) \frac{\partial C_R}{\partial z} = D_R \left[\frac{\partial^2 C_R}{\partial r^2} + \frac{1}{r} \frac{\partial C_R}{\partial r} \right] + k_f C_Z - k_b C_R, \quad (2.6)$$

$$\frac{\partial C_O}{\partial t} + v_a(r) \frac{\partial C_O}{\partial z} = D_O \left[\frac{\partial^2 C_O}{\partial r^2} + \frac{1}{r} \frac{\partial C_O}{\partial r} \right], \quad (2.7)$$

subject to

$$t = 0, \quad 0 \leq r \leq a, \quad 0 \leq z \leq l; \\ C_R = KC_Z, \quad C_R + C_Z = C^*, \quad C_O \approx 0, \quad K = \frac{k_f}{k_b}; \quad (2.8)$$

$$t > 0, \quad r = 0, \quad 0 \leq z \leq l; \\ C_R \rightarrow KC_Z, \quad C_R + C_Z \rightarrow C^*, \quad C_O \rightarrow C_O^* (\approx 0); \quad (2.9)$$

$$t > 0, \quad r = a, \quad 0 \leq z \leq l; \\ D_R \frac{\partial C_R}{\partial r} = -D_O \frac{\partial C_O}{\partial r} = -\frac{i(t)}{nFA}, \quad D_Z \frac{\partial C_Z}{\partial r} = 0. \quad (2.10)$$

(a) For reversible charge transfer reaction at the electrode surface, the boundary condition is governed by the Nernst equation:

$$t > 0, \quad 0 \leq z \leq l, \quad r = a; \\ \frac{C_R}{C_O} = \exp \left[\frac{nF}{RT} (E^0 - E(t)) \right]. \quad (2.11)$$

(b) For irreversible charge transfer reaction at the electrode surface, the boundary condition is governed by the Eyring equation:

$$t > 0, \quad r = a, \quad 0 \leq z \leq l; \\ D_R \frac{\partial C_R}{\partial r} = -D_O \frac{\partial C_O}{\partial r} = -k' C_R = -\frac{i(t)}{nFA}; \quad (2.12)$$

$$k' = k_0 \exp \left[-\frac{\alpha nF}{RT} (E(t) - E^0) \right], \quad (2.13)$$

where α is the transfer coefficient;

$$E(t) = E_i + vt, \quad (2.14)$$

where E_i is the initial electrode potential and v is the potential scan rate;

$$C_O(r, z, t) + C_R(r, z, t) + C_Z(r, z, t) = C^*. \quad (2.15)$$

The significance of various variables and parameters is given in section 5.

3. Solution

Using the same set of non-dimensional variables and parameters as in ref. [21], the model is transformed to a set of integral equations. For brevity, the assumptions and solution procedure are not repeated here and one can refer to our earlier work

where the solution is elucidated, for the EC process, in detail [21]. The set of integral equations involving concentrations of O , R , and Z are, respectively,

$$C_O = C_O^* - \int_0^{t'} f(\tau)g(\xi, t' - \tau) d\tau, \quad (3.1)$$

$$C_R = \frac{K}{1+K} \int_0^{t'} f(\tau)g(\xi, t' - \tau)(K^{-1} + e^{-\Lambda^{-2}(t'-\tau)}) d\tau, \quad (3.2)$$

$$C_Z = \frac{K}{1+K} \int_0^{t'} f(\tau)g(\xi, t' - \tau)(1 - e^{-\Lambda^{-2}(t'-\tau)}) d\tau. \quad (3.3)$$

Since it is of interest to depict the behavior of current function $f(t')$ with respect to the known behavior of potential function $E(t')$ and $E(t')$ is expressed differently in terms of concentrations for cases (a) and (b), so:

(a) *Reversible electrode charge transfer reaction*

Substituting in the Nernst equation (2.11) the expressions for C_O and C_R from equations (3.1) and (3.2), we get the following integral equation:

$$\begin{aligned} 1 - \int_0^y \chi(z)K_1(y-z) dz - \frac{1}{K} \int_0^y \chi(z)K_2(y-z) dz \\ = \frac{1+K}{K} e^{u-y} \int_0^y \chi(z)K_1(y-z) dz, \end{aligned} \quad (3.4)$$

where

$$\sigma = \frac{nFv}{RT}, \quad y = \sigma t', \quad z = \sigma \tau, \quad (3.5)$$

$$\left. \begin{aligned} \Lambda &= \left(\frac{2v_a \sqrt{D}}{al} \right)^{1/3} / \sqrt{k}, \quad k = k_f + k_b, \\ \delta &= \frac{kRT}{nFv}, \end{aligned} \right\} \quad (3.6)$$

$$u = \ln \theta = \frac{nF}{RT} (E^0 - E_i), \quad (3.7)$$

$$K_1(y, z) = \sum_{n=1}^{\infty} \frac{1}{\lambda_n} \exp \left[-\frac{\lambda_n}{\sigma} (y-z) \right], \quad (3.8)$$

$$K_2(y, z) = \sum_{n=1}^{\infty} \frac{1}{\lambda_n} \exp \left[-\left(\frac{\lambda_n}{\sigma} + \delta \right) (y-z) \right], \quad (3.9)$$

$$\chi(z) = \frac{f(z)}{C^*\sigma} = \frac{i(z)}{nFA\sqrt{kD}\Lambda C^*\sigma}. \quad (3.10)$$

(b) Irreversible electrode charge transfer reaction

Substituting in the Eyring equation (2.12) the expression for C_R from equation (3.2), we get an integral equation

$$\frac{(1+K)}{K}e^{(u-y)}\chi(y) = 1 - \int_0^y K_1(y-z)\chi(z)dz - \frac{1}{K} \int_0^y K_2(y-z)\chi(z)dz, \quad (3.11)$$

where

$$\beta = \frac{\alpha n F v}{RT}, \quad y = \beta t', \quad z = \beta \tau, \quad (3.12)$$

$$u = \ln\left(\frac{\Lambda\beta\sqrt{kD}}{k_O}\right) - \frac{\alpha n F (E_i - E^0)}{RT}, \quad (3.13)$$

$$K_1(y, z) = \sum_{n=1}^{\infty} \frac{1}{\lambda_n} \exp\left[-\frac{\lambda_n}{\beta}(y-z)\right], \quad (3.14)$$

$$K_2(y, z) = \sum_{n=1}^{\infty} \frac{1}{\lambda_n} \exp\left[-\left(\frac{\lambda_n}{\beta} + \delta\right)(y-z)\right], \quad (3.15)$$

$$\chi(y) = \frac{f(y)}{C^*\beta} = \frac{i(y)}{nFA\sqrt{kD}\Lambda C^*\beta}, \quad (3.16)$$

$$\delta = \frac{kRT}{\alpha n F v}. \quad (3.17)$$

The integral equations (3.4) and (3.11) are solved numerically using Wagner's method [22].

4. Results and discussion

In CE processes, chemical reaction preceding the electrode charge transfer reaction affects the behavior of charge transfer reaction. A non-dimensional parameter $K = (k_f/k_b)$ represents the chemical reaction in the range from perfectly reversible reaction ($K = 1$) to quasi-reversible and irreversible chemical reaction for large values of K . The effect of K on the current–potential voltammograms is studied for both reversible and irreversible charge transfer reaction schemes discussed above as cases (a) and (b), respectively. The effects of other experimentally measurable parameters, viz. the voltage scan rate and axial flow rate of the electrolyte through a tubular electrode, are also investigated.

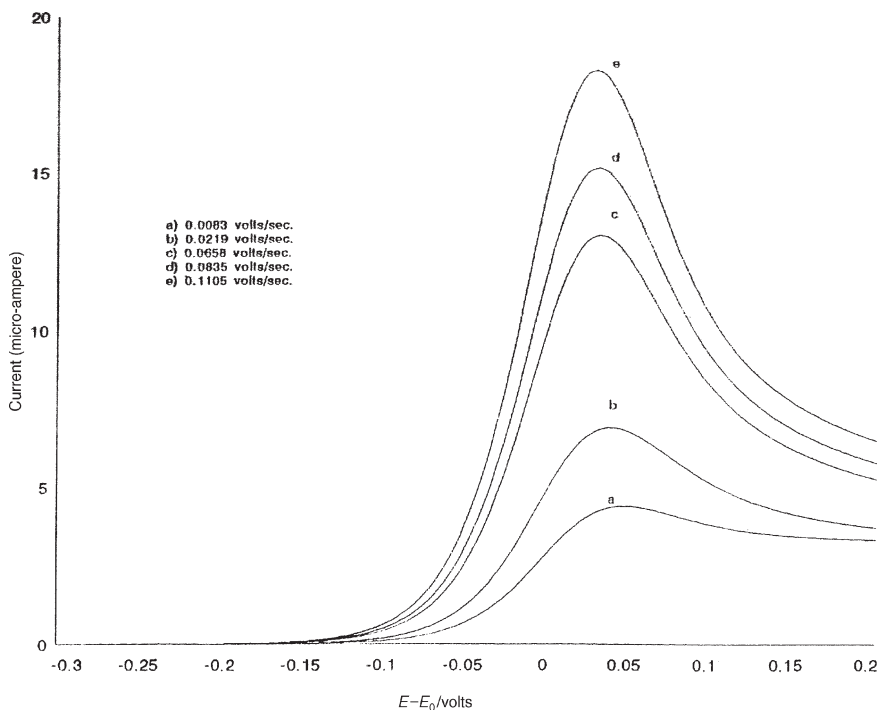


Figure 1. Current-potential curves ($K = 1$, $v_a = 0.5305$ cm/s). Variation of the scan rate.

Case (a)

The numerical solution of integral equation (3.43) gives tabulated values of $\chi(\sigma t')$ w.r.t. $\sigma t'$ whereas the current and potential are given by the equations

$$i(\sigma t') = nFA\Lambda\sqrt{kDC^*}\sigma\chi(\sigma t'), \quad (4.1)$$

$$E(t) - E^0 = \frac{RT}{nF} [(\sigma t') - u]. \quad (4.2)$$

For perfectly reversible chemical reaction ($K = 1$) and the axial flow rate of electrolyte as $v_a = 0.5305$ cm/s, the current-potential voltammograms are theoretically obtained for the variation of voltage scan rate from low values (0.0083 V/s) to high values (0.1105 V/s). The effect of such variation in scan rates results in the sharpness of the peak as well as the increase in the value of peak-current. Moreover, the peak of the C-V voltammogram shifts to the right. This is depicted in figure 1. The effect of the axial flow rate of the electrolyte through the tube on the voltammogram is depicted in figure 2. The effect of axial velocity on voltammograms is to repress the peak-current with the increase in velocity. Both these effects are justifiable since the faster rate of voltage scan will enhance the conversion of R to O and thus more current at the electrode surface which is depicted with high peak and steady-state values of the current in the voltammograms. The reverse effect is seen with the increase in

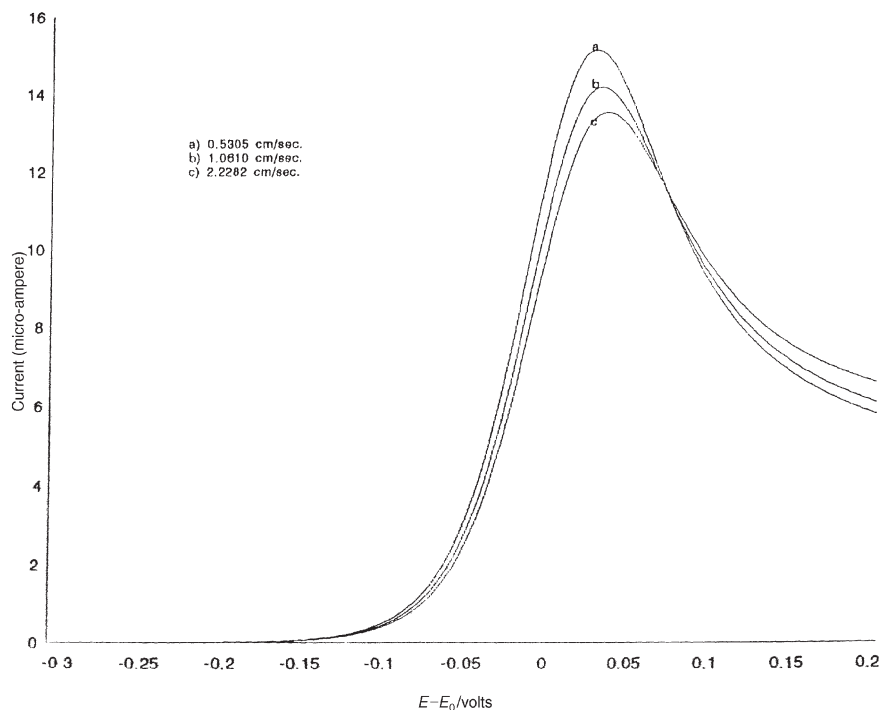


Figure 2. Current-potential curves ($K = 1$, $v = 0.0835$ V/s). Variation of the axial velocity.

axial flow rate. With higher flow rates more of electrolyte will flow out of the tubular electrode resulting in less conversion from R to O which depicts low peak-current.

In figure 3, the effect of K on peak-currents is shown. As the chemical reaction transits from perfectly reversible to quasi-reversible and then to irreversible case, the peak-current becomes sharper, indicating more of R -specie becomes available in the later case.

As the rate constants of different chemical reactions vary by many orders of magnitude, the effect of non-dimensional parameter $\delta = ((k_f + k_b)/(nFv/RT))$ on the ratio of peak current and steady-state current is studied and depicted in figure 4 as $\log \delta$ versus I_p/I_{ss} for $K = 1$ and $K = 7.5$. It is clear from the investigation that for large values of δ (approximately 1000), the ratio I_p/I_{ss} becomes static. Provided the value of chemical equilibrium constant K is known, the curves of figure 4 can be taken as working curves. From these curves, it is possible to calculate the chemical reaction rate constants k_f and k_b , after measuring peak and steady-state currents, respectively, from current-potential voltammograms.

Case (b)

A similar investigation is made for the second reaction scheme in which irreversible charge transfer reaction follows reversible chemical reaction. Where the

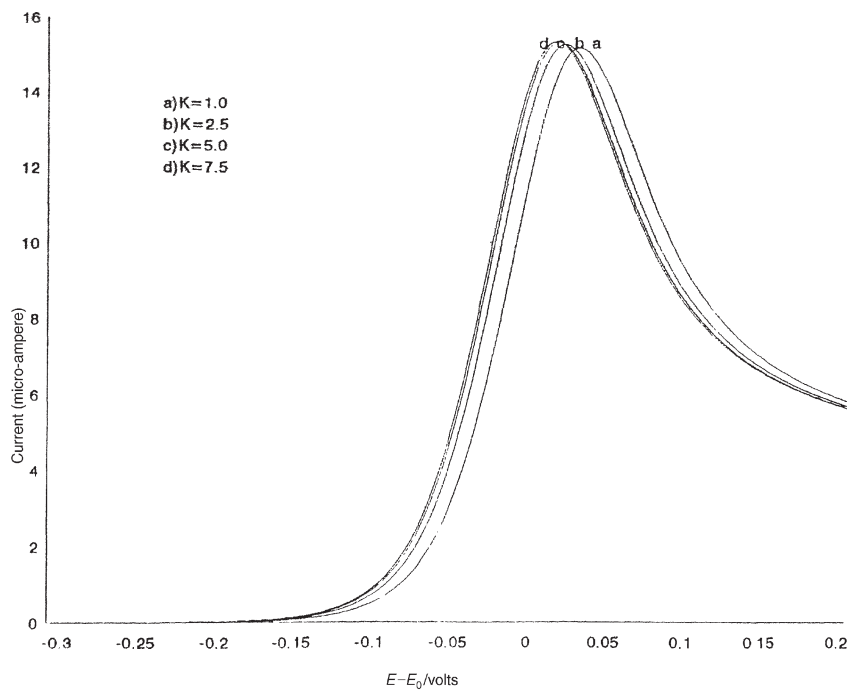


Figure 3. Current-potential curves ($v_a = 0.5305$ cm/s, $v = 0.0835$ V/s). Variation of reaction rates ratio.

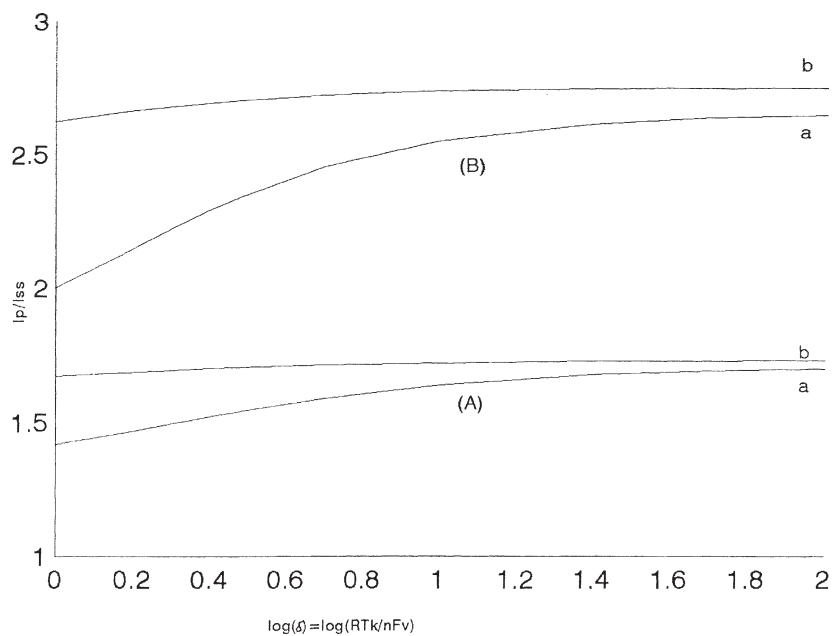


Figure 4. Variation of $\log \delta$ with I_p/I_{ss} . (A) $v = 0.0167$: (a) $K = 1$, (b) $K = 7.5$. (B) $v = 0.0835$: (a) $K = 1$, (b) $K = 7.5$.

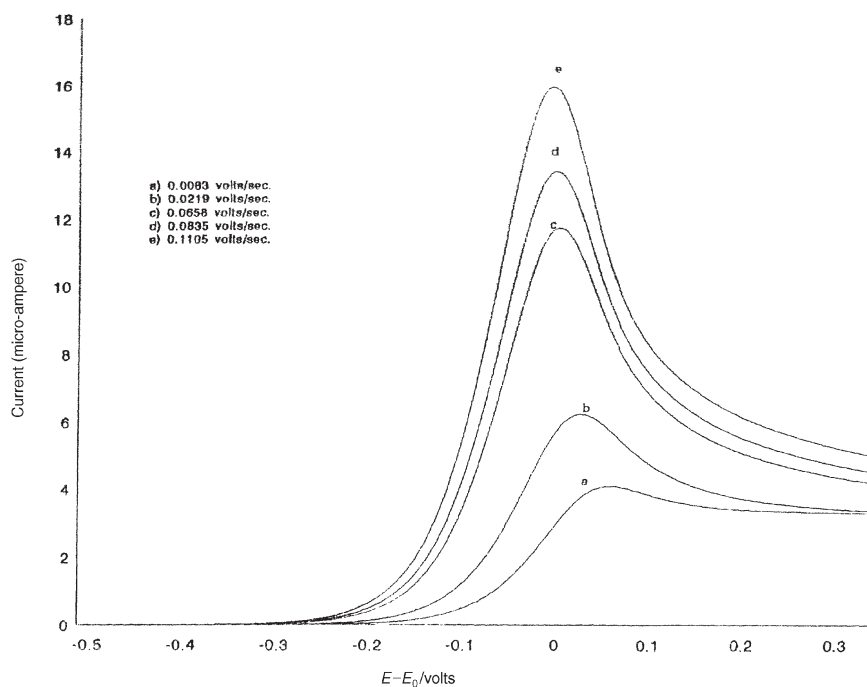


Figure 5. Current-potential curves ($K = 1$, $v_a = 0.5305$ cm/s). Variation of the scan rate.

current and potential are given by

$$i(\beta t') = nFA\Lambda\sqrt{kD}\beta C^*\chi(\beta t'), \quad (4.3)$$

$$\alpha n [E(t) - E^0] - \frac{RT}{F} \ln \frac{\Lambda\beta\sqrt{kD}}{k_0} = \frac{RT}{F} (\beta t' - u). \quad (4.4)$$

The effects of the variation of voltage scan rate and axial flow rate on current-potential voltammograms are shown in figures 5 and 6, respectively. The behavior is similar as in figures 1 and 2 but for the reverse trend of the shift of peak which is from right to left.

The effect of variation of K on the C-V curves is shown in figure 7. The peak-current is increasing with the transition from perfectly reversible to irreversible chemical reactions.

It is worth noting that the effect of the transition from perfect reversible chemical reaction to irreversible chemical reaction preceding the charge transfer reaction is depictable only if the analysis of peak currents of the C-V voltammograms is made. This is not discernible in the steady state analysis of linear sweep voltammetry.

The effect of $\log \delta (= \log((k_f + k_b)/(\alpha n F v / RT)))$ on the ratio of peak-current and corresponding steady-state current is investigated and depicted in figure 8 for two values of $K (=k_f/k_b)$. Similar trends as those for reversible electron charge transfer reaction are obtained.

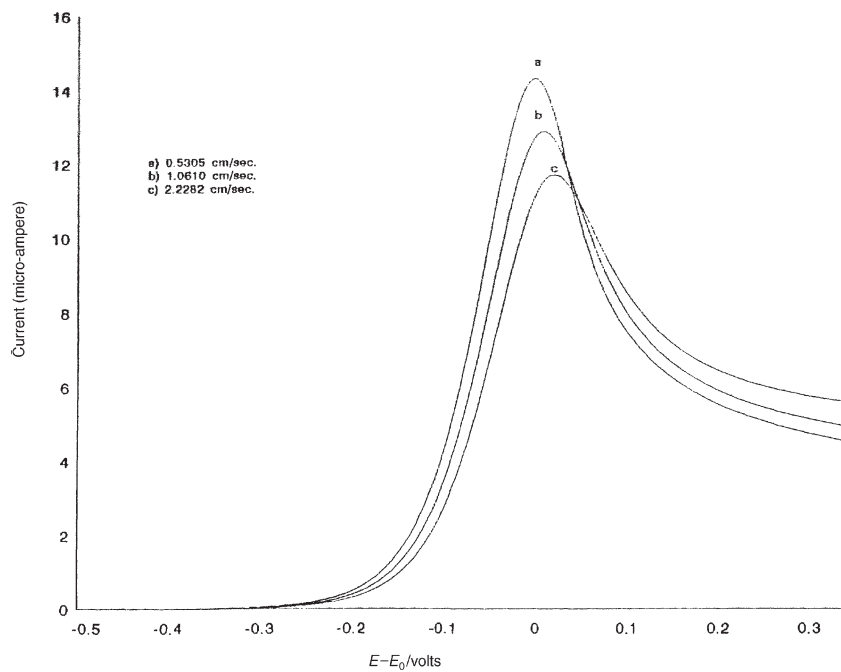


Figure 6. Current-potential curves ($K = 1$, $v = 0.0835$ V/s). Variation of the axial velocity.

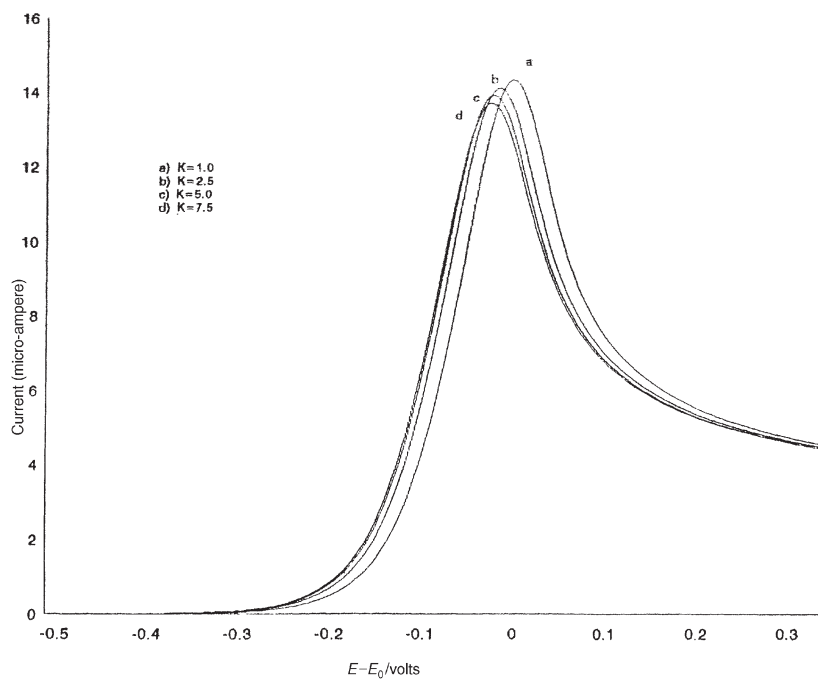


Figure 7. Current-potential curves ($v_a = 0.5305$ cm/s, $v = 0.0835$ V/s). Variation of reaction rates ratio.

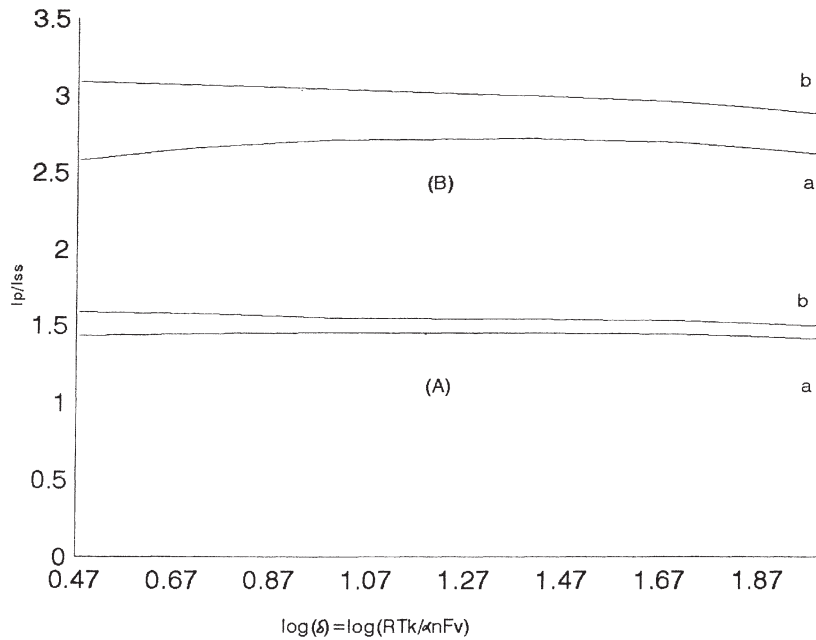


Figure 8. Variation of $\log \delta$ with I_p/I_{ss} . (A) $v = 0.0167$: (a) $K = 1$, (b) $K = 7.5$. (B) $v = 0.0835$: (a) $K = 1$, (b) $K = 7.5$.

5. Nomenclature

The values of various constants and parameters used for numerical calculations are as follows:

- a radius of the electrode (0.1 cm)
- l length of the electrode (1.0 cm)
- C_O^* initial bulk molar concentration (10^{-7} mol ml $^{-1}$)
- D diffusion coefficient (0.567×10^{-5} cm s $^{-1}$)
- R gas constant (8.31 J mol $^{-1}$ K $^{-1}$)
- T absolute temperature (298 K)
- F Faraday's constant (96487 cal mol $^{-1}$)
- E^0 standard electrode potential (-0.063 V vs. SCE)
- u parameter ($= \ln \theta$) representing the difference of initial potential E_i and standard electrode potential E^0 (8)
- v potential scan rate (0.5, 1, 3, 5 V min $^{-1}$)
- v_a axial flow velocity (0.5305, 1.0161, 1.6977 cm s $^{-1}$)
- α transfer coefficient (0.66)
- n number of electrons involved in charge transfer reaction (1)
- k_0 charge transfer rate constant (4.0×10^{-5} cm s $^{-1}$)

k_f, k_b	forward and backward chemical reaction rates ($k_f = 44.9 \text{ s}^{-1}$)
δ	$(k_f + k_b)/(nFV/RT)$, a non-dimensional kinetic parameter
K	non-dimensional chemical equilibrium parameter ($=k_f/k_b$) (1, 2, 5, 7.5)
λ_n	magnitude of n th zero of $A_1'(\eta)$ (values of first seventy zeros of $A_1'(\eta)$ are used for calculations)

Acknowledgement

The authors are thankful to the referee for his valuable suggestions and comments.

References

- [1] K. Aoki and N. Kato, *J. Electroanal. Chem.* 245 (1988) 51.
- [2] K. Aoki, K. Tokuda and H. Matsuda, *J. Electroanal. Chem.* 76 (1977) 217.
- [3] L.K. Bieniasz, *J. Electroanal. Chem.* 304 (1991) 101.
- [4] L.K. Bieniasz, *J. Electroanal. Chem.* 547 (1993) 15.
- [5] W.J. Blaedel and L.N. Klatt, *Anal. Chem.* 38 (1966) 879.
- [6] B.A. Coles and R.G. Compton, *J. Electroanal. Chem.* 127 (1981) 37.
- [7] J. Dutt and T. Singh, *Analyst* 109 (1984) 755.
- [8] J. Dutt and T. Singh, *J. Electroanal. Chem.* 182 (1985) 259.
- [9] I. Epelboin, C. Gabrielli and M. Keddam, in: *Comprehensive Treatise of Electrochemistry*, Vol. 9, *Electrodeposition: Experimental Techniques*, eds. E. Yeager, J.O.M. Bockris, B.E. Conway and S. Sarangapani (Plenum Press, New York, 1984) p. 61.
- [10] S.W. Feldberg, in: *Electroanalytical Chemistry*, ed. A.J. Bard, Series of Advances, Vol. 3 (M. Dekker, New York, 1969) p. 199.
- [11] M.S. Friedrichs, R.A. Friesner and A.J. Bard, *J. Electroanal. Chem.* 258 (1989) 243.
- [12] H. Gerisch, I. Mattes and R. Braun, *J. Electroanal. Chem.* 10 (1965) 533.
- [13] A.P. De Iribarne, S.L. Marchiano and A.J. Arvia, *Electrochim. Acta* 15 (1970) 1872.
- [14] E. Laviron, *J. Electroanal. Chem.* 52 (1974) 355.
- [15] E. Laviron, *J. Electroanal. Chem.* 101 (1979) 19.
- [16] V.G. Levich, *Physicochemical Hydrodynamics* (Prentice-Hall, Englewood Cliffs, NJ, 1962).
- [17] D.D. Macdonald, *Transient Techniques in Electrochemistry* (Plenum Press, New York, 1977).
- [18] S. Ng and H.Y. Cheh, *J. Electroanal. Chem.* 132 (1985) 93.
- [19] R.S. Nicolson and I. Shain, *Anal. Chem.* 36 (1964) 706.
- [20] T. Singh and J. Dutt, in: *Proc. 32nd Congress of ISTAM, India* (1988) p. 143.
- [21] T. Singh, R.P. Singh and J. Dutt, *J. Math. Chem.* 17 (1995) 335.
- [22] C. Wagner, *J. Math. Phys.* 32 (1954) 289.